Engineering 17 (2022) 123–139

Contents lists available at ScienceDirect

Engineering

journal homepage: www.elsevier.com/locate/eng

Research
Civil Engineering Materials—Article

Service Life Design for Concrete Engineering in Marine Environments of Northern China Based on a Modified Theoretical Model of Chloride Diffusion and Large Datasets of Ocean Parameters

Taotao Feng [a,b], Hongfa Yu [a,*], Yongshan Tan [a,c,*], Haiyan Ma [a], Mei Xu [a], Chengjun Yue [a]

[a] *Department of Civil and Airport Engineering, Nanjing University of Aeronautics and Astronautics, Nanjing 211106, China*
[b] *School of Materials Science and Engineering, Southeast University, Nanjing 211189, China*
[c] *College of Civil Science and Engineering, Yangzhou University, Yangzhou 225127, China*

ARTICLE INFO

Article history:
Received 1 December 2020
Revised 17 February 2021
Accepted 25 March 2021
Available online 8 October 2021

Keywords:
Large datasets
Modified theoretical model
Reliability theory
Service life
Boundary condition
Diffusion coefficient

ABSTRACT

In this study, through experimental research and an investigation on large datasets of the durability parameters in ocean engineering, the values, ranges, and types of distribution of the durability parameters employed for the durability design in ocean engineering in northern China were confirmed. Based on a modified theoretical model of chloride diffusion and the reliability theory, the service lives of concrete structures exposed to the splash, tidal, and underwater zones were calculated. Mixed concrete proportions meeting the requirement of a service life of 100 or 120 years were designed, and a cover thickness requirement was proposed. In addition, the effects of the different time-varying relationships of the boundary condition (C_s) and diffusion coefficient (D_f) on the service life were compared; the results showed that the time-varying relationships used in this study (i.e., C_s continuously increased and then remained stable, and D_f continuously decreased and then remained stable) were beneficial for the durability design of concrete structures in marine environment.

1. Introduction

Bohai Bay is the largest inland sea in China. The bay blocks all the cities from the northeast provinces to the eastern and southern coasts of China, which severely affects the channel for coastal passage. To alleviate this traffic situation, in 2012, the Chinese Academy of Sciences launched a research project for the construction of the Bohai Strait Cross-Sea Channel. The Bohai Strait Cross-Sea Channel connects Yantai and Dalian; the project plan entails adopting a submarine railway tunnel with a total length of 110–130 km [1]. The weather and sea conditions along the route are considerably different, which necessitates a highly durable structure. To provide a theoretical basis for the concrete mix design of the Bohai Strait Cross-Sea Channel, it is particularly important to conduct research on the durability of concrete structures in the relevant sea areas.

Dalian is located in northern China and is the end point of the Bohai Bay Cross-Sea Channel. According to the design requirements of the "Standard for durability design of concrete structures" (GB/T50476–2019) [2], the marine concrete structures in Dalian are located in a Class III marine chloride corrosion environment. Furthermore, the function grade ranges from severe (grade D) to very severe (grade E), resulting in extremely high requirements for the durability of the concrete used in these structures. Thus, a scientifically determined and reasonable durability design scheme must be formulated to ensure the safety of concrete structures in the Dalian area.

The theoretical basis for the durability analysis of concrete structures is the chloride diffusion theory based on Fick's second law, which has been widely used for the durability design of concrete structures in marine environments [3–6]. Currently, the service life design models for concrete structures are mainly improved models based on Fick's second diffusion law; among these, the most well-known models are the DuraCrete design model [7] and the Life-365 service life prediction model [8]. The DuraCrete design model is a durability design method for concrete structures based on probability, and the model formula is expressed as follows:

$$C_x = C_s\left[1 - \mathrm{erf}\left(\frac{x}{2\sqrt{K_e K_c K_M D_0 t_0^m t^{1-m}}}\right)\right] \tag{1}$$

* Corresponding authors.
E-mail addresses: yuhongfa@nuaa.edu.cn (H. Yu), ystan@nuaa.edu.cn (Y. Tan).

https://doi.org/10.1016/j.eng.2021.03.030
2095-8099/

where C_x (in mass percentage of the binders) is the chloride concentration at a certain depth x (m), C_s is the surface chloride concentration (in mass percentage of the binders), K_M is the material influence coefficient, K_e is the environmental influence coefficient, K_c is the influence coefficient of chloride diffusion, t_0 is the reference age (28 d), D_0 is the chloride diffusion coefficient at the exposure time t_0 ($m^2 \cdot s^{-1}$), m is the time-dependent index of the chloride diffusion coefficient, t is the exposure age of structural elements, and erf is the mathematical error function.

The DuraCrete design model has been successfully applied for the durability analysis of ocean engineering structures such as the Danish–Swedish Øresund Bridge [9], the submerged tunnel between the southern seashore of the Korean peninsula to an island [10], and the Hong Kong–Zhuhai–Macao sea link project in China [11]. However, the DuraCrete design model has the following characteristics: ① The model assumes that the chloride diffusion coefficient (D_t) decreases with time, whereas in practice, D_t tends to remain stable after reaching a certain age [8]; ② the model assumes that the boundary conditions remain constant, that is, C_s does not change with time, whereas in practice, C_s gradually increases with time and tends to remain stable after a certain time [12–16]; ③ the model does not consider the chloride binding capacity; and ④ the environmental influence coefficient (K_e), which affects the chloride diffusion coefficient, is obtained from short-term test data, due to which the reliability is relatively low.

The Life-365 service life prediction model [8] considers the variations in D_t and C_s with time, both of which approach constant values after varying for a certain period of time. One of the model formulas is expressed as follows:

$$C_x = k' t \left[\left(1 + \frac{x^2}{2D_t t}\right) \operatorname{erf}\left(\frac{x}{2\sqrt{D_t t}}\right) - \frac{x}{\sqrt{\pi D_t t}} \exp\left(-\frac{x^2}{4D_t t}\right) \right] \tag{2}$$

where K' is a constant.

The Life-365 service life prediction model has been applied for the durability analysis of many marine concrete structures [17,18]. However, this model uses laboratory data to evaluate the durability of concrete structures in actual environments, without considering the concrete degradation caused by the difference between indoor and outdoor environments. The chloride binding behavior is not considered either.

Yu [19] and Yu et al. [20] proposed a theoretical model of chloride diffusion in concrete based on Fick's second law; this model comprehensively accounts for various factors such as the chloride binding capacity (R_b), the time dependence of chloride diffusion (m), and the environmental effects (deterioration coefficient K). The model also resolves the long-term problem that Fick's diffusion theory is inconsistent with the actual service lives of concrete structures; this is discussed in detail in Section 2.1.

As discussed above, the durability parameters of concrete structures are directly related to the analysis results of their service life. However, thus far, research on the durability parameters of the concrete structures in Northeast Asia has been non-systematic, and the effects of the different time-varying relationships of the surface chloride concentration and chloride diffusion coefficient on the service life remain unknown. In this study, the values, ranges, and types of distribution of the durability parameters applied for the durability design in ocean engineering in northern China were confirmed. Based on the modified chloride diffusion theory and the reliability theory, the corrosion times of the steel in concrete under different service environments in the Dalian sea area were predicted with failure probabilities of 5% and 10%. The mixture proportions meeting the requirement of a service life of 100 or 120 years were determined, and a cover thickness requirement was proposed. In addition, the effects of different time-varying relationships of the boundary condition and diffusion coefficient on the service life were compared. The results of this study are expected to provide theoretical guidance for the design of marine concrete structures in northern China.

2. Theoretical model and experimental methodology

2.1. Modified theoretical model of chloride diffusion

The service life design theory for concrete structures adopted in this study was based on a modified theoretical model of chloride diffusion. The theoretical derivation process is as follows:

The basic form of the chloride diffusion equation for concrete [21] can be expressed as follows:

$$\frac{\partial C_{\text{total}}}{\partial t} = \frac{\partial}{\partial x} D_f \frac{\partial C_{\text{free}}}{\partial x} \tag{3}$$

where C_{free} is the free chloride concentration at a depth of x (in mass percentage of the concrete), C_{total} is the total chloride concentration (in mass percentage of the concrete), and D_f is the diffusion coefficient of free chloride ($m^2 \cdot s^{-1}$).

The relationship among C_{free}, C_{total}, and the bound chloride concentration (C_b) in concrete is as follows:

$$C_{\text{total}} = C_b + C_{\text{free}} \tag{4}$$

where C_b is the bound chloride concentration (in mass percentage of the concrete).

Substituting the derivative of Eq. (4) into Eq. (3) yields

$$\frac{\partial C_{\text{free}}}{\partial t} = \frac{D_f}{1 + \partial C_b / \partial C_{\text{free}}} \cdot \frac{\partial^2 C_{\text{free}}}{\partial x^2} \tag{5}$$

Chloride ions exert adsorption and binding effects on the concrete during the transport process. Tuutti [22], Arya and Newman [23], Mohammed and Hamada [24], and Yu [19] found that the chloride adsorption relationship of concrete is mainly linear:

$$C_b = R_b C_{\text{free}} \tag{6}$$

Therefore, Eq. (5) can be written as follows:

$$\frac{\partial C_{\text{free}}}{\partial t} = \frac{D_f}{1 + R_b} \cdot \frac{\partial^2 C_{\text{free}}}{\partial x^2} \tag{7}$$

Concrete, as a type of heterogeneous material, can exhibit defects such as microcracks due to external factors, including temperature stress, chemical corrosion, and freeze–thaw cycles, or internal factors, including self-shrinkage and alkali aggregate reactions. These microcracks accelerate the diffusion of chloride in the concrete. Therefore, the deterioration of concrete must be considered during theoretical modeling. A comprehensive deterioration coefficient K was introduced to describe several complex factors. K is the ratio of the diffusion coefficient of free chloride for concrete in the actual environment and the diffusion coefficient of free chloride for concrete under laboratory standard conditions; it reflects the influence of the actual service environment on chloride diffusion:

$$K = \frac{D_f}{D_{t\text{lab}}} \tag{8}$$

where $D_{t\text{lab}}$ is the diffusion coefficient of free chloride for concrete under standard laboratory conditions ($m^2 \cdot s^{-1}$).

Thomas and Bamforth [25] found that the chloride diffusion coefficient decreased exponentially with exposure time, which can be expressed as follows:

$$D_t = D_0 \left(\frac{t_0}{t}\right)^m \tag{9}$$

When the exposure condition is indoor environment, D_t is equal to D_{tlab}. By substituting Eqs. (8) and (9) into Eq. (7), the modified theoretical model of chloride diffusion can be obtained [19,20]:

$$\frac{\partial C_{\text{free}}}{\partial t} = \frac{KD_0 t_0^m}{1+R_b} \cdot t^{-m} \cdot \frac{\partial^2 C_{\text{free}}}{\partial x^2} \tag{10}$$

In an actual chloride exposure environment, the boundary condition of the modified theoretical model (i.e., C_s) does not remain constant nor does it increase continuously; instead, it changes from low to high concentration over time and gradually reaches saturation [12–16]. Xu et al. [26] performed statistical analyses on 144 groups of C_s data obtained from laboratories, on-site exposure stations, and actual engineering structures in China, Republic of Korea, Japan, the United Kingdom, the United States, Canada, and Saudi Arabia. The analysis results showed that C_s and the exposure time follow Eq. (11):

$$C_s = kt^{\frac{1-m}{2}} + C_0 \tag{11}$$

where C_0 is the initial chloride concentration in the concrete (in mass percentage of the concrete), and C_s is the surface chloride concentration, whose unit is the mass percentage of concrete when the service life analysis is carried out in this study. k is the time-dependent constant of C_s.

According to the Life-365 service life prediction model [8], the value of C_s does not increase after 7.5, 15, or 25 years (as expressed by t_1) but remains stable. In addition, in the Life-365 service life prediction model, D_f does not decrease continuously throughout the service period but instead remains stable after reaching a certain exposure time (t_2); generally, t_2 = 25 or 30 years. Fig. 1 shows the time variation laws of D_f and C_s.

Based on the time-varying relationships of C_s and D_f, the variation laws of the initial and boundary conditions can be divided into three stages:

(1) $0 < t < t_1$:

$$\begin{cases} \text{Initial condition}: t = 0, x > 0; C_{\text{free}} = C_0; \\ \text{Boundary condition}: x = 0, 0 < t < t_1; C_s = C_0 + kt^{\frac{1-m}{2}}, D_f = D_{f(t)} \end{cases}$$

(2) $t_1 \le t < t_2$

$$\begin{cases} \text{Initial condition}: t = t_1, x > 0; C_{\text{free}} = C_{\text{free}(t_1)}; \\ \text{Boundary condition}: x = 0, t_1 \le t < t_2; C_s = C_0 + kt_1^{\frac{1-m}{2}}, D_f = D_{f(t)} \end{cases}$$

(3) $t \ge t_2$:

$$\begin{cases} \text{Initial condition}: t = t_2, x > 0; C_{\text{free}} = C_{\text{free}(t_2)}; \\ \text{Boundary condition}: x = 0, t \ge t_2; C_s = C_0 + kt_1^{\frac{1-m}{2}}, D_f = D_{f(t_2)} \end{cases} \tag{12}$$

Under the initial and boundary conditions during the three stages, the calculation method for the modified theoretical model is detailed in "ChaDuraLife V1.0 life prediction model and software of concrete structures in chloride environment" [27]. For the durability analysis in this study, the reliability theory, which is typically used in engineering analyses, was adopted. The resistance factor was the critical chloride concentration (C_{cr}) of the steel, and the load effect was C_{free} on the surface of the steel. Thus, the following function can be obtained:

$$Z = C_{cr} - C_{\text{free}} \tag{13}$$

where Z is reliability function.

If $C_{cr} \le C_{\text{free}}$ is satisfied, that is, if the free chloride concentration on the steel surface reaches the critical chloride concentration, then the failure probability of the concrete structure can be obtained:

$$P_{\text{failure}} = \Phi(-\beta) \tag{14}$$

where Φ is the standard normal distribution function, P_{failure} is the failure probability, and β is the reliability index.

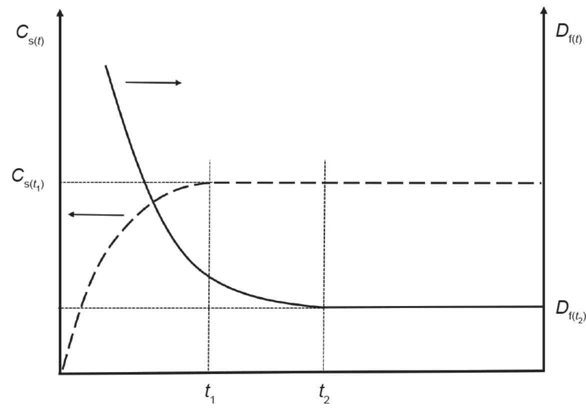

Fig. 1. Time variations of D_f and C_s.

2.2. Raw materials

P.O42.5 Portland cement was purchased from the Dalian cement plant. Class I fly ash was procured from the Dalian Huaneng Power Plant, and grade-S95 ground slag was procured from Dalian Jinqiao Company. River sand with a fineness modulus of 2.6 was used as the fine aggregate, and the coarse aggregate was local gravel from Dalian with a continuous grading of 5–25 mm. A polycarboxylate-based superplasticizer with a 26.3% water-reducing rate was used; this was obtained from Dalian Shenwei Building Materials Products Co., Ltd. Furthermore, the rosin hot polymer air-entraining agent produced by Qingdao Keli Building Materials Co., Ltd. and tap water from Dalian City were used. The mix proportions of concrete are listed in Table 1.

2.3. Specimen preparation

The raw materials, including the cement, aggregates, mineral admixtures, and admixtures, were uniformly dry mixed in a mixer for 1 min and then mixed with water for 3 min. The fresh concrete was placed into molds after mixing, vibrated for 30 s, and finally allowed to form the concrete specimens. The dimensions of the mold were 100 mm × 100 mm × 100 mm. All the test specimens were cured at room temperature for the first 24 h prior to demolding. After demolding, the specimens were cured in a standard room at a temperature of (21 ± 1) °C and a relative humidity exceeding 95%. The curing age was 28 d, and mechanical and durability tests were conducted after curing.

2.4. Exposure test and analysis method

Exposure tests were conducted after standard curing. Marine environments are complex, and seawater contains multi-component ions, as shown in Table 2. Compared with single ion transport, the electrochemical coupling effect between multiple ions has a certain influence on the transport of chloride in concrete [28–30]. Therefore, an actual marine environment was used for the exposure test. The exposure location was the prefabrication plant of CCCC First Harbor Engineering Co., Ltd. in Ganjingzi District, Dalian, adjacent to Dalian Bay. Located in the northeast, the average temperature of Dalian is 10.5 °C, with the highest temperature

Table 1
Mix proportions of concrete.

Sample	W/B	Cement ($kg·m^{-3}$)	Fly ash		Slag		Sand ($kg·m^{-3}$)	Coarse aggregate ($kg·m^{-3}$)	Water ($kg·m^{-3}$)	Superplasticizer ($kg·m^{-3}$)	Air-entraining agent ($kg·m^{-3}$)
			Mass ($kg·m^{-3}$)	Dosage (%)	Mass ($kg·m^{-3}$)	Dosage (%)					
A-1	0.34	265	66	15	110	25	688	1106	150	3.97	0.022
A-2	0.34	243	66	15	132	30	688	1106	150	3.97	0.022
A-3	0.34	221	66	15	154	35	688	1106	150	3.97	0.0265
B-1	0.32	282	70	15	117	25	660	1110	150	4.22	0.075
B-2	0.32	258	70	15	141	30	660	1110	150	4.22	0.075
B-3	0.32	235	70	15	164	35	660	1110	150	4.22	0.075
C-1	0.30	300	75	15	125	25	630	1111	150	5.00	0.090
C-2	0.30	275	75	15	150	30	630	1111	150	5.00	0.090
C-3	0.30	250	75	15	175	35	630	1111	150	5.00	0.090

W/B: water–binder ratio in weight.

Table 2
Chemical composition of seawater in Dalian Bay.

pH	Cl^- ($mg·L^{-1}$)	SO_4^{2-} ($mg·L^{-1}$)	Na^+ ($mg·L^{-1}$)	K^+ ($mg·L^{-1}$)	CO_3^{2-} ($mg·L^{-1}$)	HCO_3^- ($mg·L^{-1}$)	Ca^{2+} ($mg·L^{-1}$)	Mg^{2+} ($mg·L^{-1}$)
7.8	19 179.4	2 481.1	10 633.7	384.8	17.7	99.6	413	1 612

of 37.8 °C and the lowest temperature of −19.13 °C. The exposure environment was divided into three zones: splash, tidal, and underwater zones. Test specimens with each mixture proportion were placed in the three zones for the exposure tests, as shown in Fig. 2. Parallel exposure tests were conducted in the laboratory. Seawater obtained from Dalian Bay was used as the immersion solution, and the indoor temperature was maintained at (21 ± 1) °C.

After the specimens were cured for 28 d, their mechanical properties were tested, and compressive strength tests were conducted according to the relevant standard [31]. The specimens were drilled and sampled after exposure up to a certain age. The drill bit used was an alloy bit with a diameter of 6 mm, and the exposed cube specimens were drilled diagonally at fixed positions on two opposite sides. The sampling depths of each specimen were 0–5, 5–10, 10–15, and 15–20 mm. The coarse particles were removed using a sieve with a hole diameter of 0.16 mm, and the powdered samples from different depths in the concrete were collected. Fig. 3 shows the sampling locations of the specimens, where number 1 indicates the sampling location at the first exposure age and number 2 indicates the sampling location at the second exposure age. The total chloride ion concentration and free chloride ion concentration in the concrete were determined according to the relevant standard [32]. After the specimens were sampled, they were plugged with a mortar. The mix proportions of the mortar were the same as those of the original concrete mixture without any

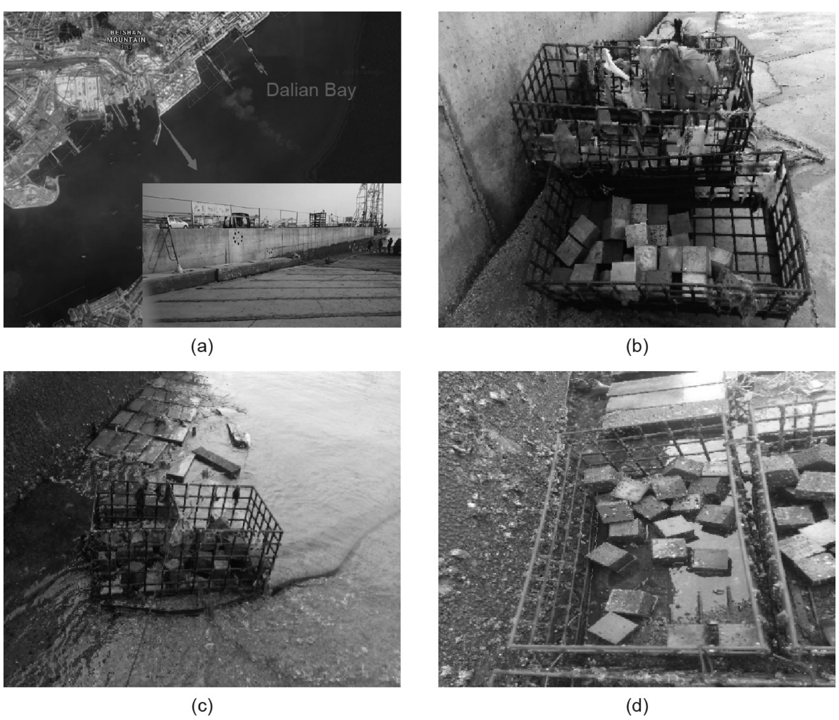

Fig. 2. Field exposure test. (a) Location of exposure station; (b) splash zone; (c) tidal zone; (d) underwater zone.

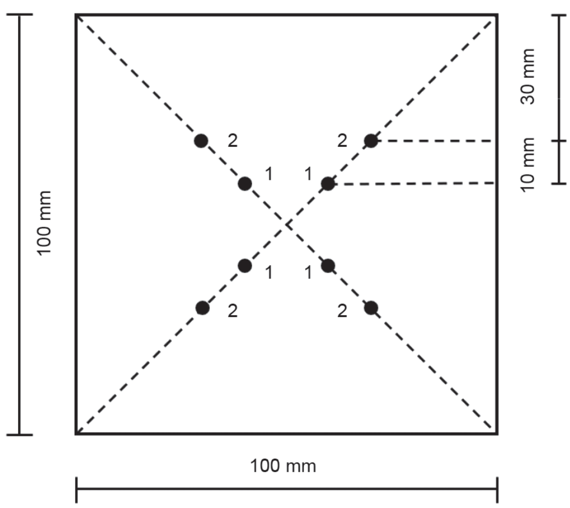

Fig. 3. Sampling locations of specimens.

coarse aggregates. After the hole was plugged for 14 d, the specimens were placed in the exposure location to continue the exposure tests. Owing to the large number of test specimens, the specific sampling times of the different specimens at each exposure age were slightly different.

3. Results and discussion

3.1. Durability parameters of marine concrete

3.1.1. Chloride diffusion coefficient (D_0) and time-dependent index (m)

Table 3 shows the compressive strengths of the samples with different mix proportions, and the variations in the chloride concentrations of the specimens immersed in indoor seawater are shown in Fig. 4. C_{free} decreased quadratically with the diffusion depth. The method adopted for calculating the C_s value is as follows. Using regression analysis for the C_{free} values at average depths of 2.5, 7.5, 12.5, and 17.5 mm, a quadratic function relating C_{free} and the diffusion depth was obtained. By setting the diffusion depth to 0 in the regression formula, the C_s value was obtained.

Yu [19] and Yu et al. [33,34] established a chloride diffusion model in a finite body with a constant homogeneous boundary condition based on a three-dimensional condition, as follows:

$$C_{\text{free}} = C_s + \sum_{i=1,3,5}\sum_{j=1,3,5}\sum_{q=1,3,5}\frac{64}{ijq\pi^3}(C_0 - C_s) \cdot \sin\left(\frac{i\pi}{L_1}x\right)\sin\left(\frac{j\pi}{L_2}y\right)\sin\left(\frac{q\pi}{L_3}z\right)\cdot\exp\left[-D_t\left(\frac{i^2\pi^2}{L_1^2}+\frac{j^2\pi^2}{L_2^2}+\frac{q^2\pi^2}{L_3^2}\right)t\right] \quad (15)$$

where L_1, L_2, and L_3 are the lengths of concrete specimens in the x-, y-, and z-directions (mm), respectively.

Using Eq. (15), the chloride diffusion coefficient of concrete at exposure time t can be obtained. The $D_{t\text{lab}}$ values for each mix proportion at different exposure times are listed in Table 4.

Table 3
Cube compressive strengths for different mix proportions (MPa).

Sample	A-1	A-2	A-3	B-1	B-2	B-3	C-1	C-2	C-3
Compressive strength	55.2	56.6	55.6	58.2	55.0	63.6	57.4	67.4	58.2

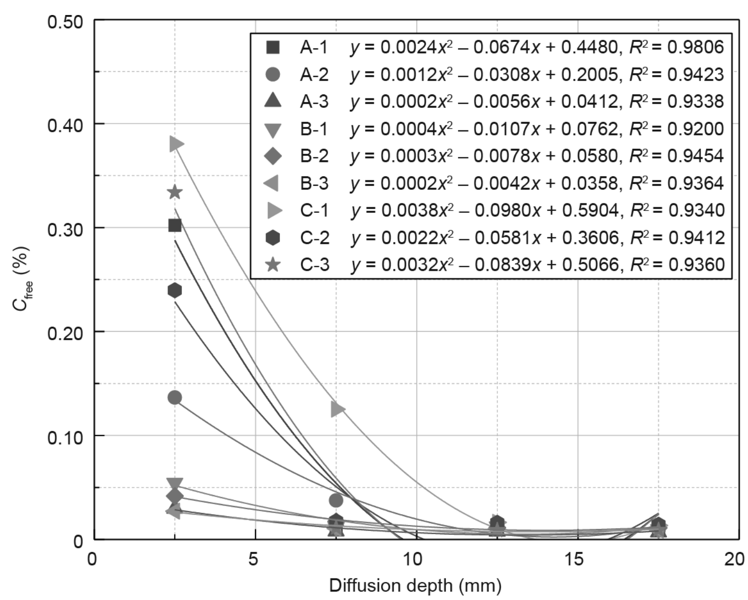

Fig. 4. Diffusion of C_{free} under indoor natural diffusion conditions.

Table 4
$D_{t\text{lab}}$ for different mixture proportions.

Sample	A-1	A-2	A-3	B-1	B-2	B-3	C-1	C-2	C-3
t (d)	220	200	188	200	200	185	218	218	220
$D_{t\text{lab}}$ ($\times10^{-12}$ m^2·s^{-1})	0.657	0.669	0.660	0.633	0.630	0.655	0.586	0.549	0.519

During the durability design and service life analysis of a concrete structure, the reliability of the calculation results is determined based on the reasonability of each parameter. Yu et al. [34] investigated the chloride concentration data collected from 2207 marine exposure stations and practical projects in 20 countries. The temporal variation in D_t was systematically studied, and a universal m value of 0.6304 was proposed, as shown in Fig. 5. The number of concrete samples was sufficiently large and the exposure time span was wide (7 d to 91 years); hence, it was reasonable to select this m value for the service life design. Combined with the D_{tlab} values at different exposure times, shown in Table 4, and the value of the long-term time-dependent index m (0.6304), the chloride diffusion coefficient at 28 d (D_0) could be obtained based on the diffusion coefficient evolution formula (Eq. (9)). The specific results are presented in Table 5. It is evident from the results that the chloride diffusion coefficient of concrete under the same water–binder ratio decreases with an increase in the slag content, indicating that slag can reduce the chloride diffusion coefficient of concrete; this is consistent with the conclusions of many studies [35–37].

3.1.2. Chloride binding capacity (R_b)

Through chemical analyses, the C_{free} and C_{total} values for the different mix proportions were obtained. Using Eqs. (4) and (6), the relationship between C_{free} and C_{total} was obtained, as shown in Eq. (16), and the R_{b} value could then be obtained. Fig. 6 shows the C_{free} and C_{total} results for each mix proportion, as obtained from the chemical analyses. Furthermore, using regression analysis, R_{b} was determined to be 0.36.

$$C_{\mathrm{total}} = (1 + R_{\mathrm{b}})C_{\mathrm{free}} \tag{16}$$

3.1.3. Critical chloride concentration (C_{cr})

C_{cr} refers to the critical chloride concentration that can destroy the passive film of the steel surface; it is of great significance for durability analyses in ocean engineering [38]. In the durability design and analysis of several large-scale marine structures built in China over recent years, the C_{cr} values have been systematically discussed and analyzed. Jin et al. [39] analyzed and predicted the service life of the Jiaozhou Bay subsea tunnel, and the C_{cr} value was set to 0.85% (accounting for the mass fraction of the cementitious material). In the design process of the Hong Kong–Zhuhai–Macao Bridge, the C_{cr} values were as follows: 0.85% in the atmospheric zone, 0.75% in the splash and tidal zones, and 2.00% in the underwater zone (accounting for the mass fraction of the cementitious materials) [11,40].

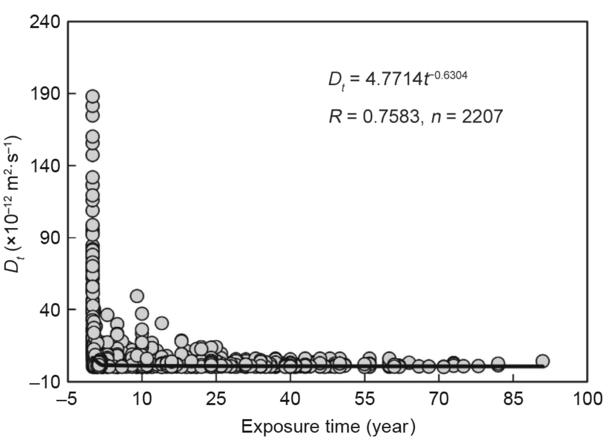

Fig. 5. Temporal changes in D_t [34] (n is sample number).

Table 5
D_0 for different mix proportions.

Sample	A-1	A-2	A-3	B-1	B-2	B-3	C-1	C-2	C-3
D_0 ($\times10^{-12}$ $\mathrm{m^2 \cdot s^{-1}}$)	2.41	2.31	2.19	2.18	2.17	2.15	2.14	2.00	1.90

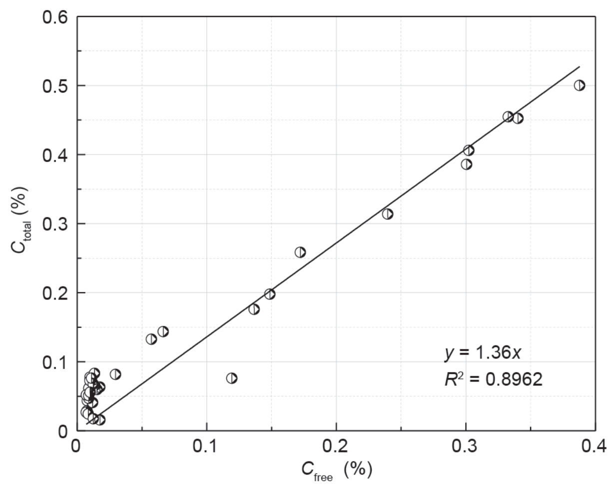

Fig. 6. Chloride binding capacity.

To study the C_{cr} characteristics of concrete structures in the Dalian sea area, the corrosion status of a steel bar in a concrete wharf, with a service life of 40 years near Songmu island in Dalian, was investigated. The concrete cover thickness was 60 mm, and the wharf was located in the tidal zone. Five concrete core samples were drilled, and the average value of C_{free} on the surface of the steel at the concrete cover was found to be 0.13% (accounting for the concrete mass fraction) by using chemical analyses in accordance with the relevant standard [32]. The steel was removed from the core sample, and there is no corrosion at the surface of the steel bar, as shown in Fig. 7. Thus, the C_{cr} value is greater than 0.13%. Combined with the above mentioned research results and safety considerations, a relatively conservative value of 0.13% (accounting for the concrete mass fraction) was used as the C_{cr} value in the splash and tidal zones. Owing to the low oxygen content in the saturated water environment, the cathode reaction could not proceed smoothly during steel corrosion. Therefore, the steel bars in the underwater zone are less prone to rust, as compared to those in the splash and tidal zones [41,42]. Compared with those in the splash and tidal zones, the C_{cr} value in the underwater zone could be slightly larger. Therefore, 0.15% of the mass fraction of concrete was used. By converting the C_{cr} values into mass fractions of the cementitious materials for the A-3, B-3, and C-3 mix proportions, the C_{cr} values in the splash zone (tidal zone) were approximately 0.70%, 0.66%, and 0.62%, respectively, while the C_{cr} values in the underwater zone were approximately 0.81%, 0.76%, and 0.72%, respectively. These values are all slightly lower than those in the literature mentioned above and would yield relatively conservative estimates for the service life design of concrete structures in marine environments.

3.1.4. Degradation coefficient (K)

The deterioration coefficient reflects the effect of concrete deterioration on the chloride diffusion under the influence of the external environment. To analyze the service life of concrete structures, the differences in the chloride diffusion coefficients between the

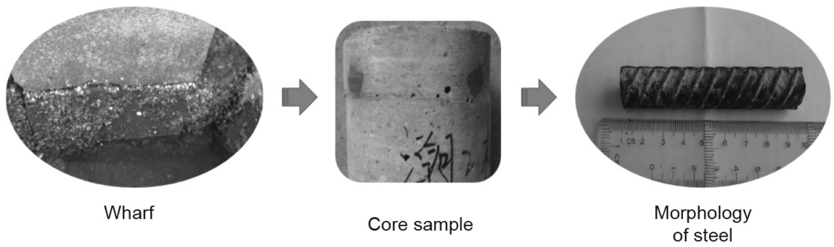

Fig. 7. Corrosion status of steel in a concrete wharf with a service age of 40 a in Dalian.

indoor and outdoor concretes were analyzed. In addition, data related to the marine concrete structures in the Dalian area were investigated. By combining these results, the values of K could be determined. For the exposure experiments, the chloride concentration tests under different exposure environments were divided based on two exposure ages. Owing to the large number of test specimens, for the same mix proportion, the specific exposure times under different exposure environments were slightly different, as shown in Table 6.

Fig. 8 shows the chloride diffusion rules for all the mix proportions under the indoor and field exposure environments. According to the chloride diffusion theoretical model (Eq. (15)), the D_f values for the different mix proportions in the actual service environment were calculated. Compared with the corresponding D_{tlab} values under the laboratory standard conditions, the values of K in the Dalian marine environment were subsequently determined. Although there were some differences in the specific exposure times, considering that the differences in the diffusion coefficients were small when the exposure times approached one another, the small differences in the specific exposure times could be neglected. Therefore, the K values under different exposure environments were calculated directly using Eq. (8). For a small number of test specimens, the exposure times under the indoor and field exposure environments were significantly different (marked with * in Table 6), and these specimens were not considered in the calculation of K. The calculation results are listed in Table 7. Through a statistical analysis of the data in Table 7, the average K values for the concrete in the Dalian sea area were determined to be 1.61 for the splash zone, 1.58 for the tide zone, and 1.59 for the underwater zone, and the corresponding standard deviations were 0.85, 0.94, and 0.87, respectively. Feng [43] calculated the K values of a wharf constructed using high-performance concrete, which had been in service for 11 a in the Dalian area, and determined values of 1.52 for the splash area and 1.32 for the tidal area and that the variation coefficient did not exceed 20%. The test K values were similar to the long-term data obtained from the site. Therefore, the K values used for the service life design of concrete structures in the Dalian area were as follows: 1.61 for the splash zone, 1.58 for the tidal zone, and 1.59 for the underwater zone.

3.1.5. Time-dependent constant of surface free chloride concentration (k)

To determine the values of k, long-term data regarding the concrete surface chloride concentration (C_s) of wharfs with service times of 11, 28, 40, 50, and 82 years in the Dalian area and data from ocean engineering or exposure stations in Northeast Asia were collected. In some reports, the total surface chloride concentration ($C_{s(total)}$) is presented instead of the free surface chloride content ($C_{s(free)}$). To unify the results, the $C_{s(total)}$ values were converted to $C_{s(free)}$ using Eq. (17), which was proposed by Xu et al. [26]:

$$C_{s(free)} = 0.9092 C_{s(total)} \ (n = 471, \ R = 0.9586) \tag{17}$$

The statistical results for the $C_{s(free)}$ values of marine concrete after conversion are presented in Table 8 [44–53]. After combining the time-varying model of C_s (Eq. (11)) and a previously proposed universal time-dependent index of the diffusion coefficient (m = 0.6304) [34], a regression analysis was performed considering different exposure environments, in which C_0 was generally 0.01% [54]. The fitting relationship is shown in Fig. 9, and the specific values of the fitting parameters are listed in Table 9. The results show that C_s increased with increasing exposure time. Furthermore, upon fitting according to the $(1-m)/2$ power-law boundary condition, the fitted value of k was 0.2567 for the splash zone and 0.2885 for the tidal zone. However, for the underwater zone, the amount of data in Table 8 was relatively small and was not representative; thus, it could not be used directly in the durability analysis. Because the environment of the tidal zone is closer to that of the underwater zone than to that of the splash zone, the boundary condition of the tidal zone was used to determine the service life of the marine concrete structures in the underwater zone.

Table 6
Specific exposure times for different concrete samples (d).

Exposure age	Exposure environment	A-1	A-2	A-3	B-1	B-2	B-3	C-1	C-2	C-3
First age	Indoor	81	81	109	101	82	82	82	137	137
	Splash zone	81	–	103	117	–	81	132*	132	130
	Tidal zone	78	78	103	113	118*	78	131*	132	130
	Underwater zone	–	81	103	112	112*	81	130*	131	131
Second age	Indoor	220	200	188	200	200	188	218	218	220
	Splash zone	187*	187	–	–	–	181	211	–	–
	Tidal zone	186*	187	–	214	214	180	–	195*	195*
	Underwater zone	185*	187	195	207	210	182	208	207	204

"–" indicates that the case was untested. "*" indicates that the exposure times under the indoor and field exposure environments were significantly different.

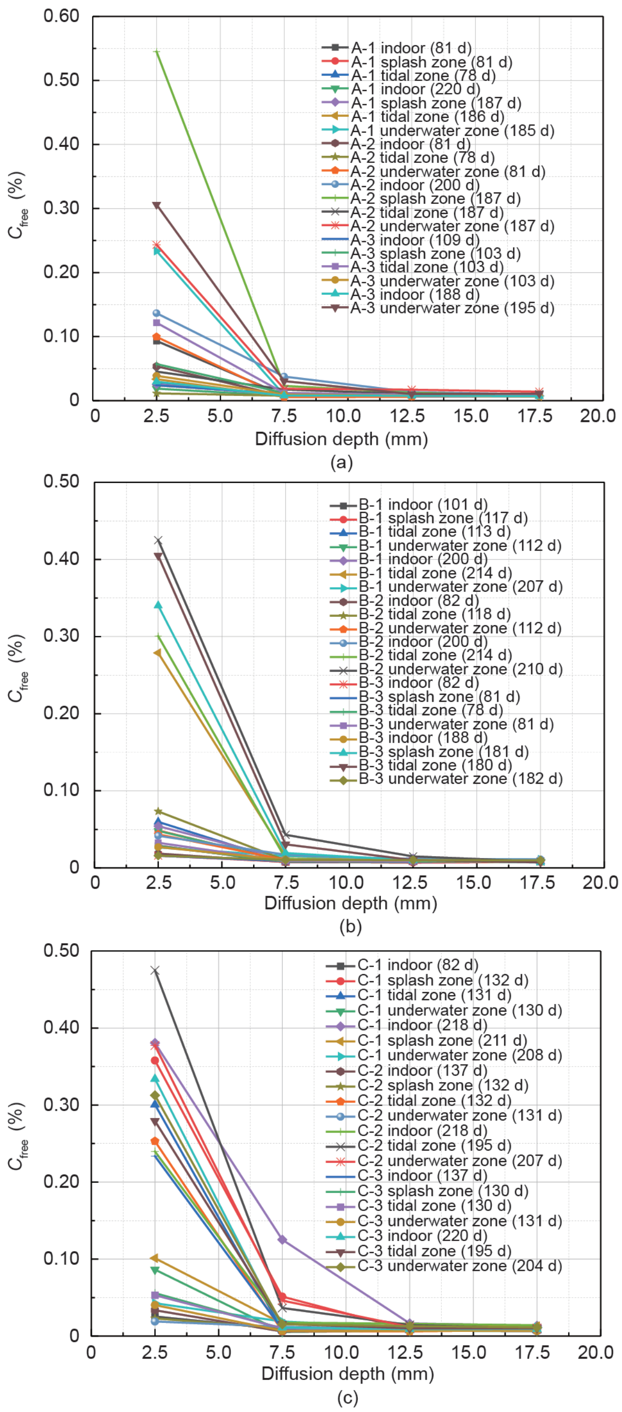

Fig. 8. Chloride diffusion in concrete under different exposure environments. (a) A series; (b) B series; (c) C series.

Table 8
Literature values of $C_{s(free)}$ for marine concrete.

Exposure zone	Service time (year)	$C_{s(free)}$ (%)	Data source
Splash zone	11	0.3937	[44]
	40	0.5552	
	50	0.6651	
	82	0.6240	
	30	0.6204	[45]
	2	0.2060	[46]
	2	0.2091	
	4	0.2660	
	4	0.2219	
	4	0.3589	
	73	0.3644	[47]
	11	0.3241	[48]
	27	0.3177	
	22	0.3930	[49]
	39	0.6169	[50]
	39	0.6290	
	39	0.3945	
	39	0.4228	
	35	0.4511	
	40	0.6088	
	40	0.5926	
	19	0.3622	
	19	0.5684	
	19	0.5158	
	19	0.4956	
	21	0.5926	
	21	0.4228	
	29	0.6088	
Tidal zone	11	0.5857	[44]
	28	0.6816	
	40	0.8644	
	82	0.4621	
	0.65	0.2277	[51]
	0.65	0.2809	
	0.65	0.2425	
	0.65	0.2661	
	0.65	0.2691	
	2.22	0.2425	
	2.22	0.2661	
	2.22	0.2824	
	8.99	0.3148	
	8.99	0.2735	
	22.54	0.3030	
	44.36	0.4167	
	48.65	0.4137	
	16	0.4667	[52]
	16	0.6837	
	16	0.5930	
	40	0.6286	
	40	0.8381	
	40	0.7107	
	41	0.7323	
	22	0.4262	[49]
Underwater zone	21	0.6516	[53]
	23	0.9199	
	25	1.0559	
	73	1.0073	[47]
	73	1.1492	
	73	1.2244	

Table 7
Deterioration coefficient (K) of concrete in the Dalian marine environment.

Exposure age	Exposure environment	A-1	A-2	A-3	B-1	B-2	B-3	C-1	C-2	C-3
First age	Splash zone	1.97		1.25	0.85		3.67		1.76	1.59
	Tidal zone	0.98	2.12	3.36	0.90		1.14		1.22	1.66
	Underwater zone		2.63	1.01	1.17		0.99		0.91	1.53
Second age	Splash zone		0.99				1.07	1.36		
	Tidal zone		3.27		1.06	0.90	0.82			
	Underwater zone		1.11	1.12	3.98	1.04	2.29	2.05	1.19	1.19

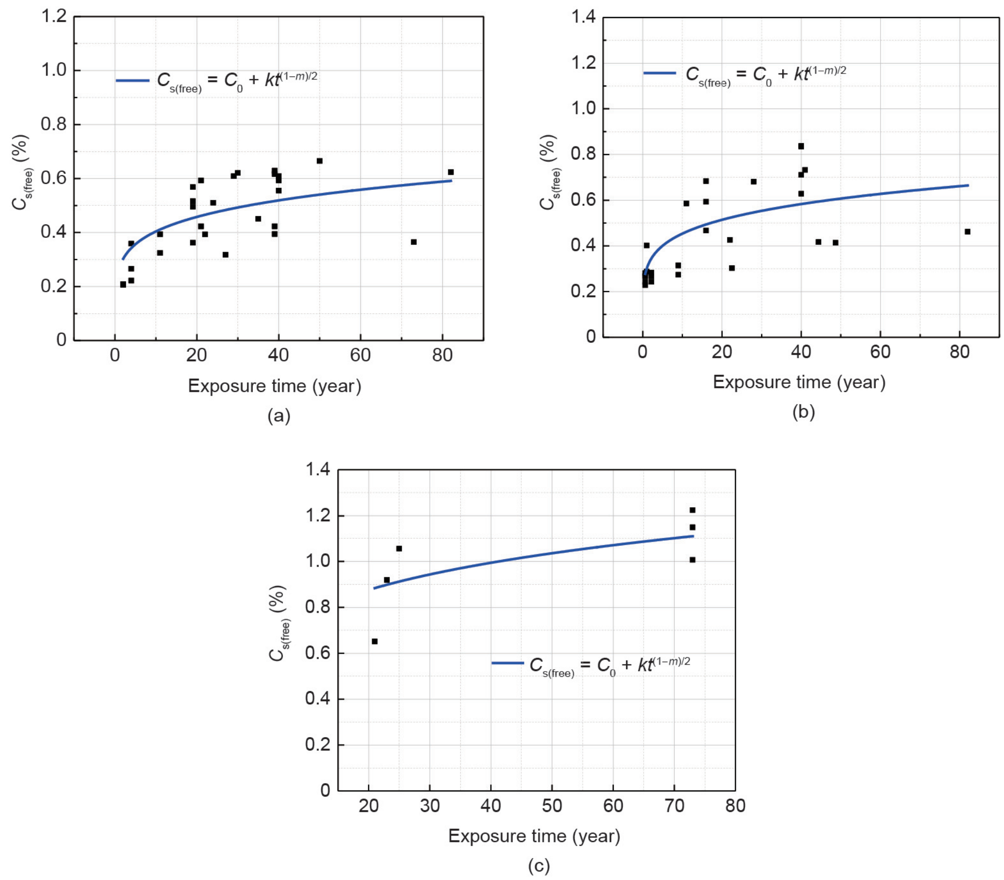

Fig. 9. Temporal variations in $C_{s(free)}$ in different exposure zones. (a) Splash zone; (b) tidal zone; (c) underwater zone.

Table 9
Regression analysis results for time-varying forms of $C_{s(free)}$ in different exposure zones.

Exposure zone	Parameter values	Correlation coefficient R	Sample number	Critical correlation coefficient R^*
Splash zone	C_0 = 0.01%, m = 0.6304, k = 0.2567	0.7025	28	0.6618
Tidal zone	C_0 = 0.01%, m = 0.6304, k = 0.2885	0.7129	24	0.6880
Underwater zone	C_0 = 0.01%, m = 0.6304, k = 0.4979	0.7129	6	–

Significance level of critical correlation coefficient R^* with α = 0.02.

3.2. Distribution types of durability parameters

3.2.1. Statistics of distribution types of model parameters

In the reliability analysis of the service lives of marine concrete structures, the accuracy of the calculation results is related to the distribution types of each parameter in the design model, such as the cover thickness x_0, C_s, and D_0. Therefore, the statistical distribution types of model parameters must be systematically analyzed. Table 10 [10,40,55–68] summarizes the distribution types of the model parameters for a large number of marine concrete struc-

Table 10
Statistics of probability distribution types of model parameters in the literature.

Model parameters	Distribution type								
	Normal distribution	Lognormal distribution	Uniform distribution	Beta distribution	Weibull distribution	Generalized extremum distribution	Gumbel distribution	Truncated distribution	Constant
x_0	[10,40,55–63]	[57,64,65]		[10,66–68]					
C_s	[55–57,59,61,62,66–68]	[40,57,60,53–65]				[10]			
C_0									
C_{cr}	[55–57,59,61,66–68]	[57,65]	[64]	[40,57,60,62,63]			[10]		
D_0	[40,55–58,60,61,63,66–68]	[57,59,64,65]			[10]				
m	[10,40,55–57,59,60,66–68]			[62,63]				[61]	[57,65]
K	[10,66–68]								

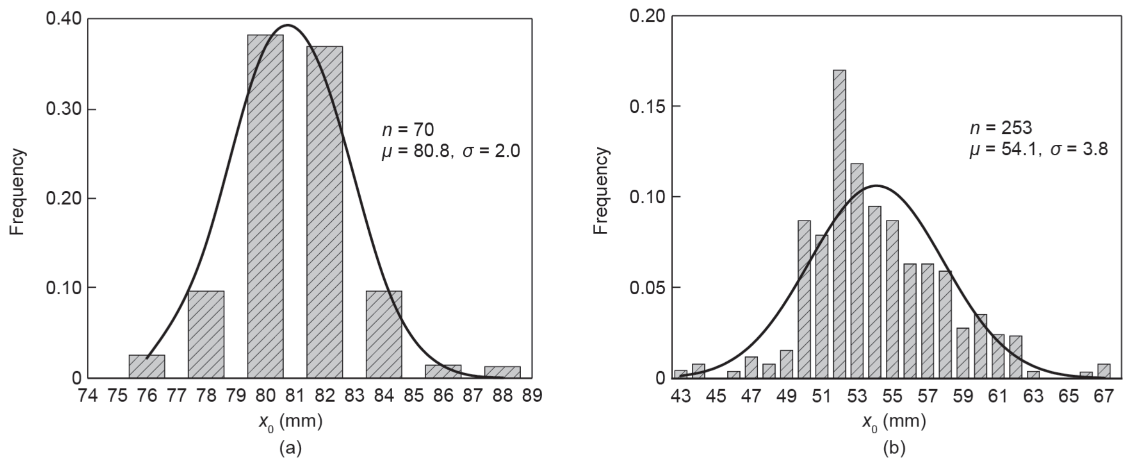

Fig. 10. Quality control level for different design cover thicknesses: (a) 80 mm and (b) 50 mm. μ: average value; σ: standard deviation.

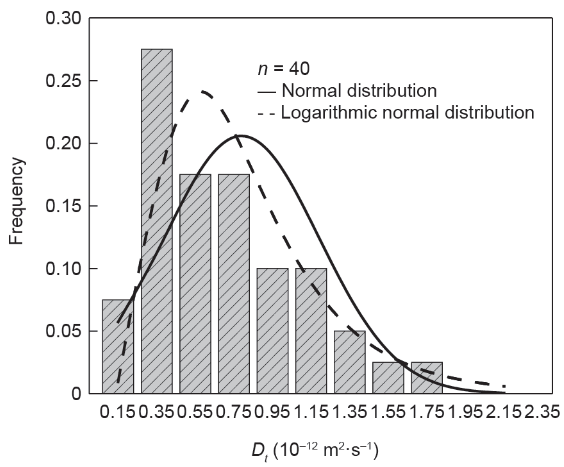

Fig. 11. Quality control level for D_t.

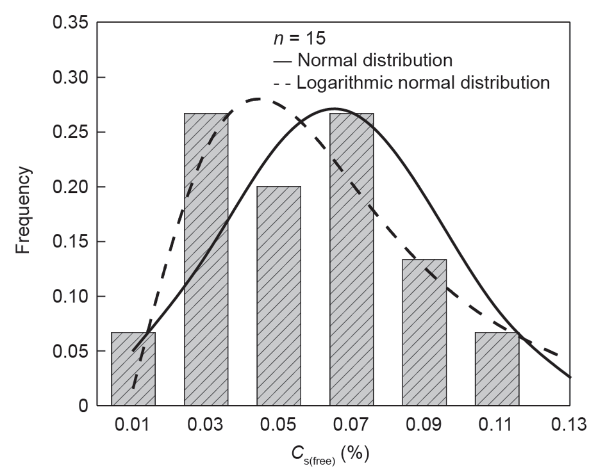

Fig. 12. Quality control level for $C_{s(free)}$.

tures. Most previous studies have shown that the durability parameters mainly follow normal distributions.

3.2.2. Quality control level of construction firm

(1) Cover thickness (x_0)

The control of the cover thickness and durability parameters of concrete is mainly related to the management level of the construction firm. Fig. 10 shows the statistical distributions of the cover thickness of the marine concrete structures constructed in recent years by CCCC First Harbor Engineering Bureau Third Engineering Co., Ltd., which has undertaken many seaport projects in the Dalian area. Fig. 10(a) shows the cover thickness of a concrete structure with a design cover thickness of 80 mm at the 317# berth at Dandong Port. Fig. 10(b) shows the cover thicknesses of ① the CX7-2# caisson and breast wall of the outfitting wharf at Dalian Zhongyuan Kawasaki Shipping Engineering Co., Ltd.; ② the caisson at the 22# berth of the Phase IV Project on the North Bank of Dayao Bay, Dalian Port; ③ the berth breast wall of Dandong Port; and ④ the breast wall of the 72# berth at Yingkou Port, which have the design cover thickness of 50 mm. The statistical results showed that when the design cover thickness was 80 mm, the average value of the actual cover thickness was 80.8 mm, the standard deviation was 2.0 mm, and the variation coefficient was 2.5%. When the design cover thickness was 50 mm, the average value of the actual cover thickness was 54.1 mm, the standard deviation

Table 11
Model parameters of service life analysis.

Model parameters	Average values	Distribution types	Remark
C_0 (%)	0.01	N (0.01, 0.002)	Mass fraction of concrete
D_0 ($\times 10^{-12}$ $m^2 \cdot s^{-1}$)	2.19	N (2.19, 0.44)	A-3
	2.15	N (2.15, 0.43)	B-3
	1.90	N (1.90, 0.38)	C-3
t_0 (d)	28		
t_1 (year)	15		
t_2 (year)	30		
R_b	0.36	N (0.36, 0.07)	
k	0.2567	N (0.2567, 0.0513)	Splash zone
	0.2885	N (0.2885, 0.0577)	Tidal and underwater zone
m	0.6304	N (0.6304, 0.1261)	
K	1.61	N (1.61, 0.85)	Splash zone
	1.58	N (1.58, 0.94)	Tidal zone
	1.59	N (1.59, 0.87)	Underwater zone
C_{cr} (%)	0.13	N (0.13, 0.026)	Splash and tidal zone (mass fraction of concrete)
	0.15	N (0.15, 0.030)	Underwater zone (mass fraction of concrete)
x_0 (mm)	70	N (70, 14)	

N: normal distribution; the two data in the parentheses are the average value and standard deviation, respectively.

was 3.8 mm, and the variation coefficient was 7.0%. Regardless of its design value, the concrete cover thickness essentially follows a normal distribution.

(2) Chloride diffusion coefficient (D_t)

Fig. 11 shows the quality control level for the D_t values of a batch of concrete specimens prepared by CCCC First Harbor Engineering Bureau Third Engineering Co., Ltd. The D_t values can be considered to follow both normal and lognormal distributions. For convenience of analysis, a normal distribution was used to analyze the service life in this study.

(3) Surface free chloride concentration ($C_{s(free)}$)

Fig. 12 shows the quality control level for the $C_{s(free)}$ values of a batch of concrete specimens prepared by CCCC First Harbor Engineering Bureau Third Engineering Co., Ltd. The results show that the $C_{s(free)}$ values follow both normal and lognormal distributions. To ensure convenient reliability calculation, a normal distribution was used to analyze the service life in this study.

3.2.3. Determination of distribution types of model parameters

Based on results reported in the literature (Table 10) and the quality control level of the construction firm, the durability parameters of the service life design model were observed to exhibit mainly normal distributions. Studies on the initial chloride concentration C_0 are still relatively limited, and it was assumed to follow a normal distribution in this study. Therefore, in the theoretical model of the service life design, except for the exposure time (which was a constant), the other parameters were all random variables with normal distributions. The variation coefficients of k, C_0, C_{cr}, R_b, x_0, m, and D_0 were all set as 20%. For the variation coefficient of K, test values were used based on the differences between

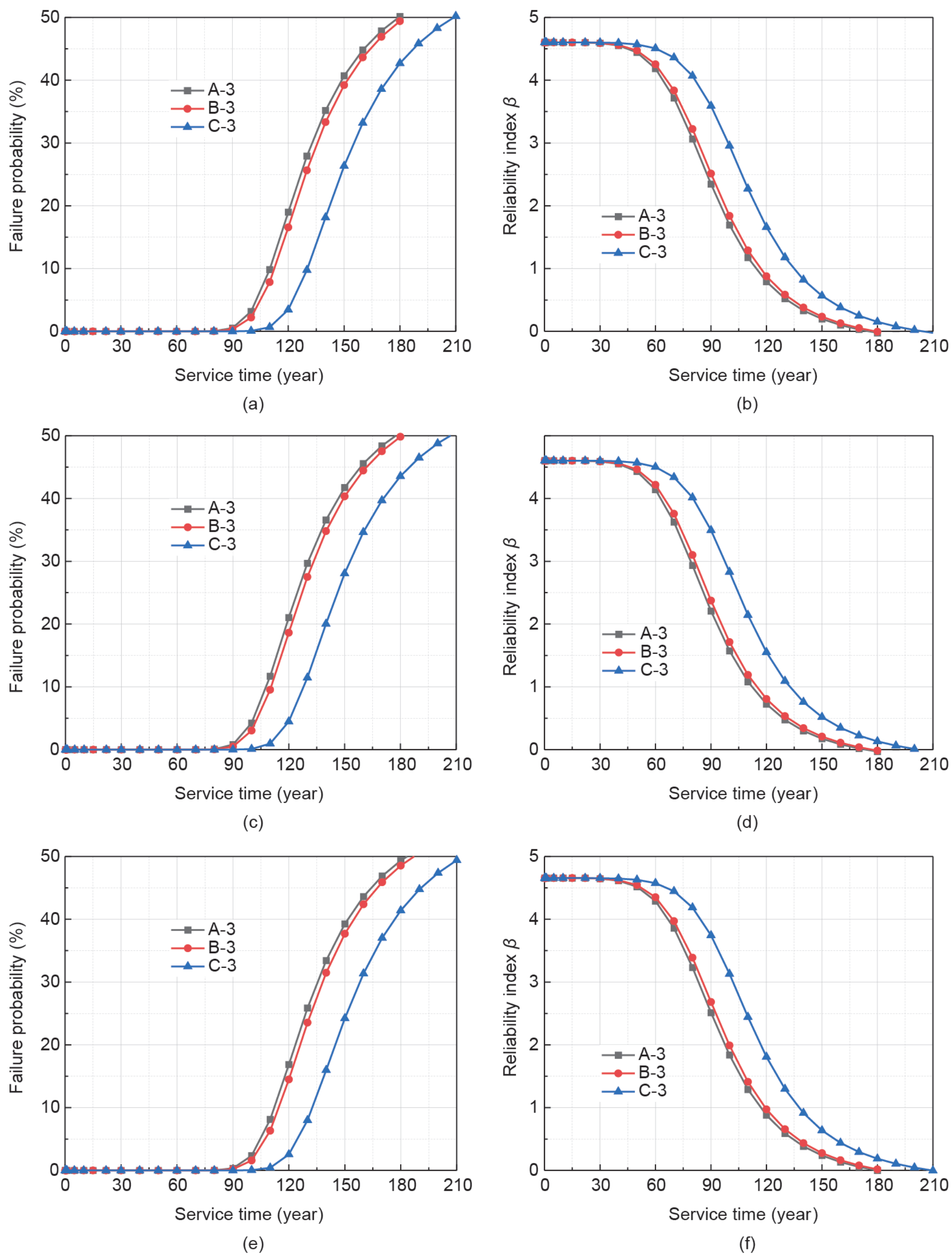

Fig. 13. Corrosion probability of steel and reliability index in different service environments: (a, b) splash zone; (c, d) tidal zone; and (e, f) underwater zone.

Table 12
Corrosion time of steel in concrete structures under different service environments.

Sample	Service time (year)					
	Corrosion probability of 5%			Corrosion probability of 10%		
	Splash zone	Tidal zone	Underwater zone	Splash zone	Tidal zone	Underwater zone
A-3	102	101	105	110	107	112
B-3	105	102	106	112	110	115
C-3	122	121	126	130	127	132

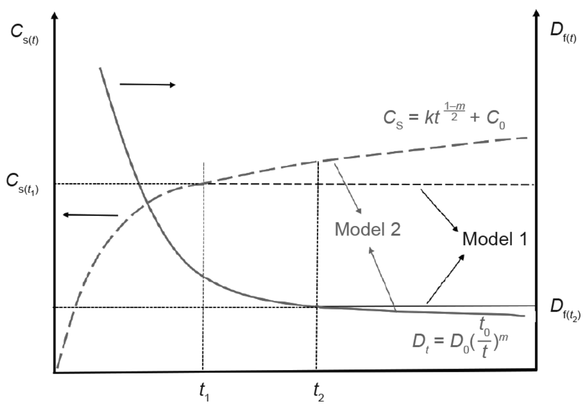

Fig. 14. Different time-varying relationships of boundary conditions and diffusion coefficient.

the marine exposure environments. The design value of x_0 was 70 mm. The values and distribution types of the durability parameters of the service life analysis model are listed in Table 11.

The "Standard for Design of Concrete Structure Durability" (GB/T 50476–2019) [2] stipulates that the design service life of a structure corresponding to the durability limit state should have a specified assurance rate and meet the reliability requirements of the normal service limit state. According to the standard, the structural reliability range is 90%–95%, and the corresponding failure probability is 5%–10%. Therefore, in this study, the service time was defined as the time when the corrosion probability (i.e., failure probability) of the steel bars in concrete reached 5% and 10%, respectively.

3.3. Reliability analysis of service life of marine concrete structures

3.3.1. Service life analysis of concrete structures in different exposure environments

Fig. 13 and Table 12 show the corrosion probability of the steel inside concrete structures and the corresponding reliability index in different exposure zones. With the extension of the service time, the failure probability increased, and the reliability index decreased gradually. For the concrete structures in the splash zone, the service lives of the A-3, B-3, and C-3 mix proportions were 102, 105, and 122 year, respectively, when the corrosion probability was 5%, and they were 110, 112, and 130 year, respectively, when the corrosion probability was 10%. All mix proportions met the 100-year-life design requirement, and the C-3 concrete met the 120-year-life design requirement. For the concrete structures in the tidal zone environment, the service lives of the A-3, B-3, and C-3 mix proportions were 101, 102, and 121 a, respectively, when the corrosion probability was 5%, and they were 107, 110, and 127 year, respectively, when the corrosion probability was 10%. Although the service lives were lower than those in the splash zone, all the mix proportions still met the 100-year-life design requirement, and the service life of C-3 reached 120 year. For the concrete structures in the underwater zone, the service lives of the A-3, B-3, and C-3 mix proportions were 105, 106, and 126 a, respectively, when the corrosion probability was 5%, and they were 112, 115, and 132 year, respectively, when the corrosion probability was 10%. Based on the aforementioned results, A-3 concrete could be used for marine concrete structures with a 100-year design life, and C-3 concrete could be used for structures with a 120-year design life. Furthermore, the service life was shortest in the tidal zone and longest in the underwater zone. Therefore, analyzing the durability of marine concrete structures based on the service environment in the tidal zone yields reliable and conserva-

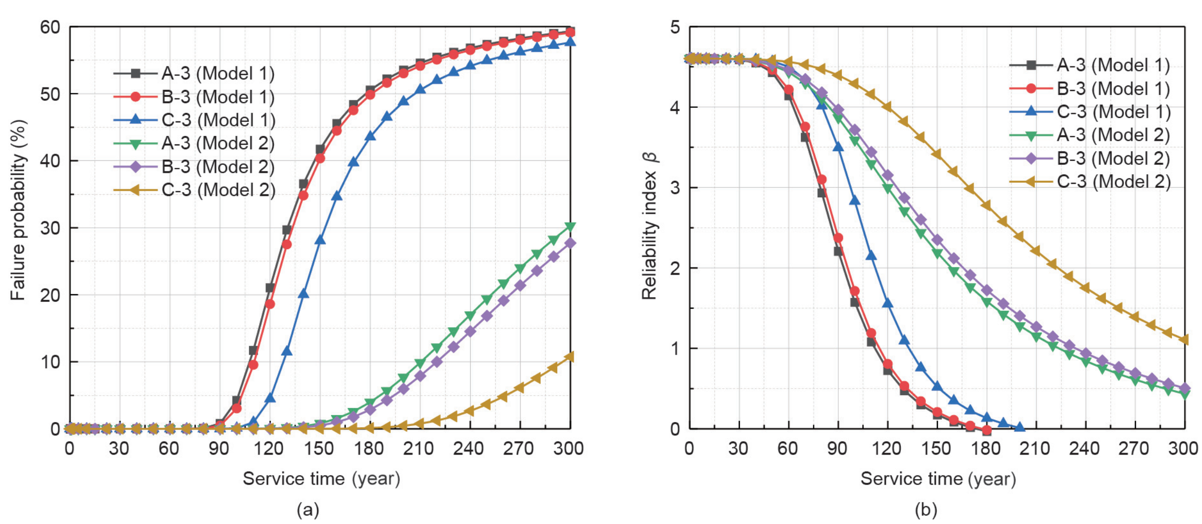

Fig. 15. Comparison of (a) corrosion probabilities and (b) reliability indices under two calculation conditions. Model 1: D_f decreases first and then remains stable, and C_s increases first and then remains stable; Model 2: C_s continuously increases and D_f continuously decreases.

Table 13
Rust times (year) of steel bars under two types of calculation conditions.

Sample	Continuous change in C_s and D_f		C_s and D_f remain stable after reaching a certain age	
	Corrosion probability of 5%	Corrosion probability of 10%	Corrosion probability of 5%	Corrosion probability of 10%
A-3	185	210	101	107
B-3	195	220	102	110
C-3	262	295	121	127

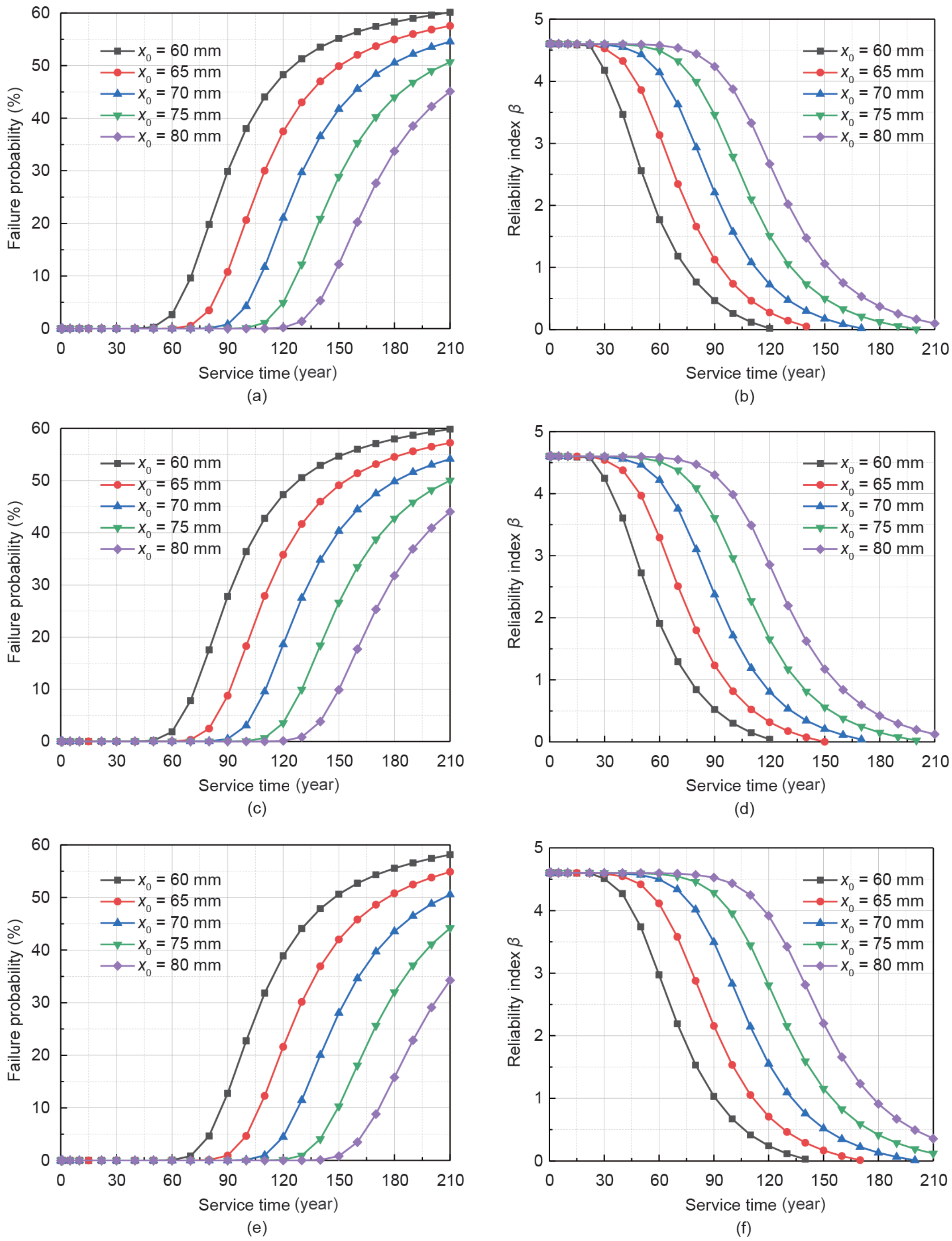

Fig. 16. Comparison of corrosion probabilities and reliability indices of concrete structures with different cover thicknesses: (a, b) A-3; (c, d) B-3; and (e, f) C-3.

tive results. Thus, to facilitate manufacturing and quality control, the tidal zone was selected as the environmental basis for the design of marine concrete structures.

3.3.2. Difference in service life of marine concrete structures—continuous increase in C_s and continuous decrease in D_f

In the service life analysis of the marine concrete structures, the time-varying relationships between D_f and C_s were considered; specifically, C_s continuously increased and then remained stable after t_1, while D_f continuously decreased and remained stable after t_2 (Model 1). With C_s continuously increasing and D_f continuously decreasing (Model 2), as shown in Fig. 14, the calculation result for the service life might change to some extent. To clarify the influence of the model differences on the service life, the service life calculations based on different boundary conditions and chloride diffusion behaviors are discussed below.

The service lives of the marine concrete structures with different mix proportions were recalculated with the tidal zone as the service environment. Fig. 15 shows the corrosion probability and the corresponding reliability index. The service lives of the A-3, B-3, and C-3 mix proportions were 185, 195, and 262 year, respectively, when the corrosion probability was 5%, and 210, 220, and 295 year, respectively, when the corrosion probability was 10%. The specific service lives are listed in Table 13. During the service life of the structure, even if C_s continuously increases and D_f continuously decreases, the predicted service lives are 83.2%–116.5% (average 97.0%) and 96.0%–132.3% (average 109.6%) longer than that of model 1 (with C_s continuously increasing and then remaining stable, and D_f continuously decreasing and then remaining stable) for corrosion probabilities of 5% and 10%, respectively. Evidently, these two effects would not cause the actual engineering life to be lower than the expected service life. Considering that C_s continually increases and then remains stable after t_1 and that D_f continually decreases and then remains stable after t_2, the results are conservative and reliable, which is beneficial for the durability design of marine concrete structures.

3.3.3. Cover thickness of concrete structures calculated in tidal zone

The thickness of the concrete cover significantly influences the service life of marine concrete structures. According to the calculation results presented earlier, when the concrete cover thickness was 70 mm, the A-3, B-3, and C-3 mix proportions could ensure that the steel would not rust within 100 or 120 year, even in the tidal zone (in which the conditions were relatively severe). To ensure compliance with the design requirement in terms of service life, the service lives of the marine concrete structures were examined with the cover thickness varying from 60 to 80 mm in increments of 5 mm, for the A-3, B-3, and C-3 mix proportions in the tidal zone environment.

Fig. 16 and Table 14 show the corrosion probabilities of the steels and the corresponding reliability indices for different cover thicknesses. The results show that the corrosion time increased with an increase in the concrete cover thickness. For a 5% corrosion probability, the corrosion times of the A-3, B-3, and C-3 concrete structures were 81, 82, and 91 year, respectively, when the cover thickness was 65 mm; these values do not meet the design requirements of 100 or 120 year. However, when the cover thickness was 70 and 75 mm, the corrosion times were 101, 102, and 121 year, respectively, and 120, 121, and 141 year, respectively. With an increase in the cover thickness, the rusting time of the steels increased further. According to the requirements mentioned in the JTG/T B07-01–2006 standard [69], the design value of the cover thickness should not be less than the sum of the minimum cover thickness and the permitted construction error Δ. The Δ was determined based on the strictness of the construction requirements, and a range of 0–5 mm was used for the prefabricated components. Assuming that the concrete structures were produced using the precast construction method, the Δ value of the cover thickness was 5 mm, and the minimum thickness was 70 mm according to the calculation results presented earlier. Therefore, the suggested cover thickness was $x_0 \geq 75$ mm. This meets the requirement of the JTS151–2011 standard, which states that "the minimum concrete cover thickness of the load-bearing bars of reinforced concrete structures is 60 mm" [70].

3.3.4. Sensitivity analysis based on C_s in tidal zone to calculate service life of concrete structures in underwater zone

Because the available statistical data for C_s in the underwater zones of Dalian and Northeast Asia are limited, the C_s data in the tidal zone, which is similar to the underwater zone, was selected in this study to calculate the service life of concrete structures in the underwater zone. To analyze the influence of selecting these values on the service life, the sensitivity of C_s in the tidal zone to

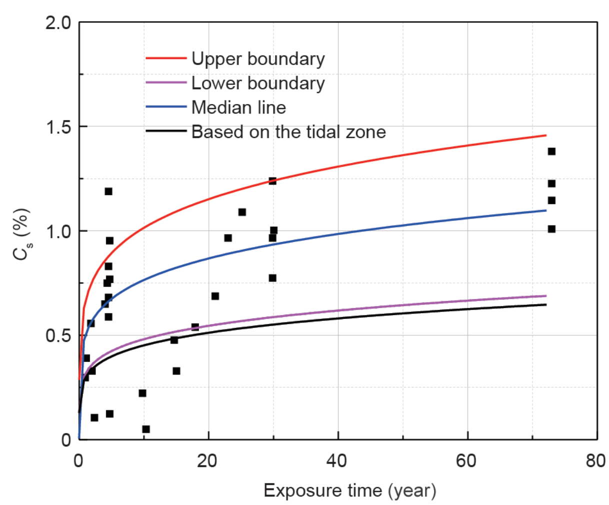

Fig. 17. Temporal variation in C_s in underwater zone in a global scale.

Table 14
Corrosion time (year) of steels in concrete structures with different cover thicknesses (x_0).

x_0 (mm)	Corrosion probability of 5%			Corrosion probability of 10%		
	A-3	B-3	C-3	A-3	B-3	C-3
60	62	62	80	70	72	84
65	81	82	91	85	91	107
70	101	102	121	107	110	127
75	120	121	141	126	130	147
80	136	141	161	146	150	171

the service life of the structures in the underwater zone was determined using the temporal variations in C_s in underwater zones on a global scale. The data points in Fig. 17 denote the statistical results of the C_s values in marine underwater zones on a global scale [25]; the exposure age ranged from 1 to 72 year. A regression analysis of C_s for a large number of marine concrete structures revealed that the majority of the C_s values in the underwater zone were between the upper and lower boundaries, as shown in Fig. 17. Using Eq. (11), the boundary condition functions of the upper boundary, lower boundary, and median line were obtained, and the corresponding k values were 0.6562, 0.3076, and 0.4930, respectively. Although the fitting degree was not sufficiently high, the purpose was to analyze the influence of the difference in k caused by the exposure environment on the service life. The detailed calculation results for the service life under different boundary conditions are shown in Fig. 18 and Table 15 for a cover thickness of 75 mm.

The calculation results show that when the C_s of the marine concrete structures was located on the middle line in Fig. 16, the service life was approximately 87.6%–89.7% of the life calculated based on the tidal zone. When the C_s was at the lower boundary, the service life was very close to the calculated result for the tidal zone. When the C_s of the actual engineering structure was at the upper boundary, which is the most unfavorable condition, the service life was approximately 80.2%–84.1% of the life calculated based on the tidal zone. For the A-3 and C-3 concrete, even when the C_s was located on the upper boundary, the rust times of the steel bars reached 101–107 and 121–127 years, respectively, for a failure probability of 5%–10%; thus, the service life design requirements of 100 and 120 a were fulfilled. Although the data for the tidal zone were selected as the calculation basis, the service life could still meet the design requirements if the structures were located in the underwater zone.

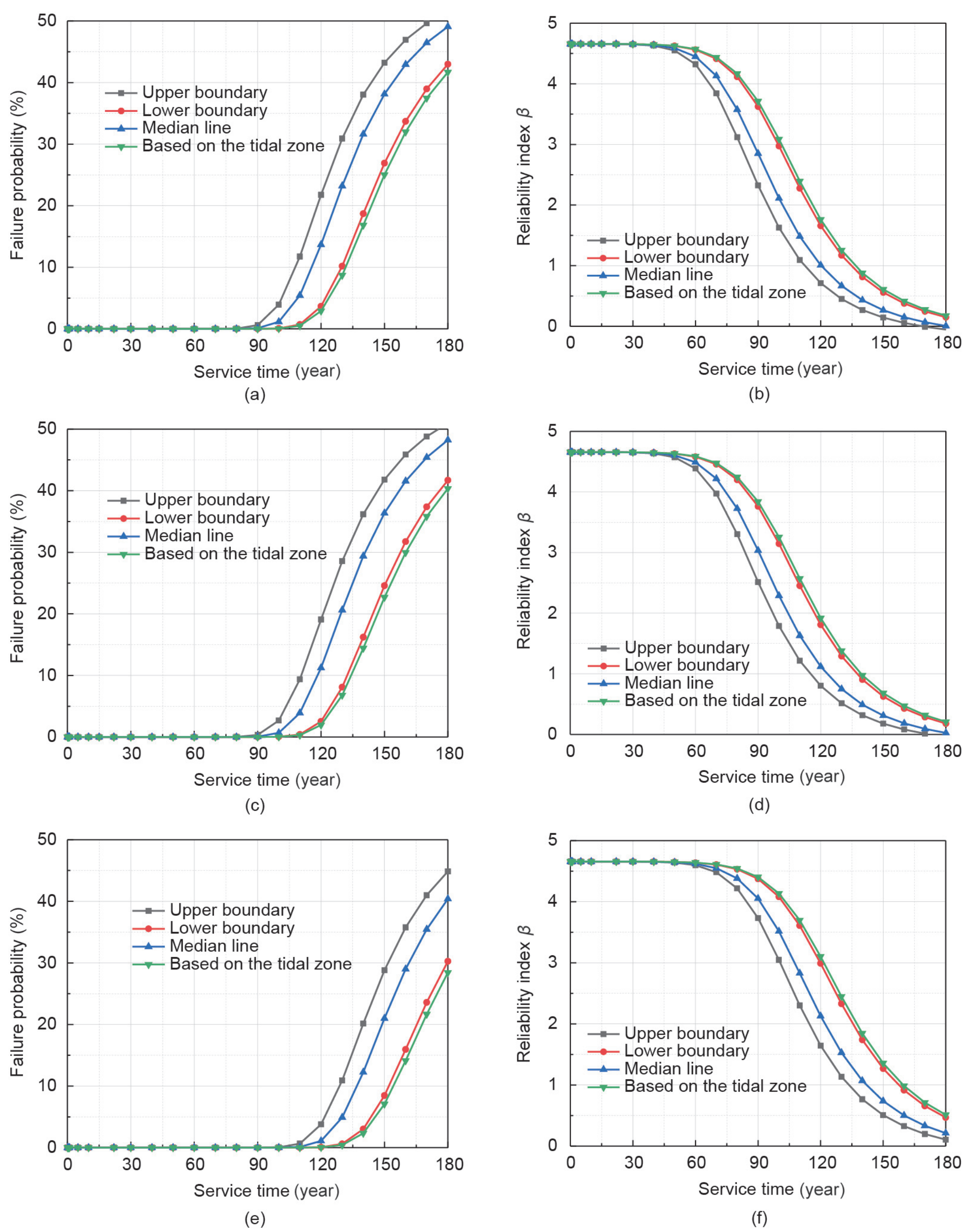

Fig. 18. Corrosion probability and reliability index of concrete structures under different boundary conditions: (a, b) A-3; (c, d) B-3; and (e, f) C-3.

Table 15
Possible deviation in service life of concrete structures in the underwater zone.

Sample	Failure probability (%)	Underwater zone (year)			Based on tidal zone (year)
		Upper boundary (year)	Lower boundary (year)	Median line (year)	
A-3	5	101	121	106	121
	10	107	128	116	131
B-3	5	101	125	111	126
	10	111	131	117	132
C-3	5	121	141	130	145
	10	127	151	136	155

4. Conclusions

The service lives of concrete structures in northern China were analyzed based on large datasets of ocean parameters and on reliability theory. A design method was proposed to ensure a service life of 100 or 120 years. The main conclusions are as follows:

(1) Through experimental research and investigation of large datasets of durability parameters used in ocean engineering, the values, ranges, and distribution types of the durability parameters applied in the durability design of marine concrete structures in northern China were confirmed.

(2) Based on the modified theoretical model of chloride diffusion in concrete and reliability theory, the service lives of concrete structures exposed to splash, tidal, and underwater zones were calculated. Accordingly, mix proportions that would achieve a service life of 100 or 120 years were designed.

(3) The influence of the cover thickness on the service life was analyzed, and $x_0 \geq 75$ mm was suggested to be an appropriate cover thickness for marine concrete structures in northern China.

(4) The service life of marine concrete structures was analyzed and compared under two time-varying relationships of D_f and C_s (D_f continuously decreasing and C_s continuously increasing; D_f first decreasing and then remaining stable, and C_s first increasing and then remaining stable). When C_s continuously increased and then remained stable and D_f continuously decreased and then remained stable, the results were conservative and reliable, which is beneficial for the durability design of concrete structures.

Acknowledgments

The authors gratefully acknowledge the financial support provided by the Natural Science Foundation of China (51508272, 11832013, 51878350, and 51678304).

Compliance with ethics guidelines

Taotao Feng, Hongfa Yu, Yongshan Tan, Haiyan Ma, Mei Xu, and Chengjun Yue declare that they have no conflict of interest or financial conflicts to disclose.

References:

[1] Wang M, Song K. Urgency and current construction conditions and preliminary scheme of Bohai Strait cross-sea channel. J Beijing Jiaotong Univ 2013;37:1–10. Chinese.
[2] Ministry of Housing and Urban–Rural Developments of the People's Republic of China. GB/T 50476–2019: Standard for design of concrete structure durability. Chinese standard. Beijing: China National Standard; 2019. Chinese.
[3] Shi X, Xie N, Fortune K, Gong J. Durability of steel reinforced concrete in chloride environments: an overview. Constr Build Mater 2012;30:125–38.
[4] Meira GR, Andrade C, Padaratz IJ, Alonso Jr C, Borba Jr JC. Chloride penetration into concrete structures in the marine atmosphere zone-relationship between deposition of chlorides on the wet candle and chlorides accumulated into concrete. Cement Concr Compos 2007;29(9):667–76.
[5] Oh BH, Jang SY. Effects of material and environmental parameters on chloride penetration profiles in concrete structures. Cement Concr Res 2007;37(1):47–53.
[6] Li K, Zhang D, Li Q, Fan Z. Durability for concrete structures in marine environments of HZM project: design, assessment and beyond. Cement Concr Res 2019;115:545–58.
[7] Brite EuRam III. General guideline for durability design and redesign: DuraCrete—probabilistic performance based durability design of concrete structures. Report. Brussel: European Union; 2000 Feb. Report No. 32155789/87. Contract No. BRPR-CT95-0132.
[8] Thomas MDA, Bentz EC. Life-365, service life prediction model, computer program for predicting the service life and life-cycle cost of reinforced concrete exposed to chlorides. Toronto: University of Toronto; 2001.
[9] Janssen W, Lykke S. The fixed link across the Øresund: tunnel section under the Drogden. Tunn Undergr Space Technol 1997;12(1):5–14.
[10] Song HW, Pack SW, Ann KY. Probabilistic assessment to predict the time to corrosion of steel in reinforced concrete tunnel box exposed to sea water. Constr Build Mater 2009;23(10):3270–8.
[11] Wang S, Su Q, Fan Z, Li Q, Zhou X, Li K. Durability design principle and method for concrete structures in Hong Kong–Zhuhai–Macao sea link project. Chin Civil Eng J 2014;47:1–8. Chinese.
[12] Amey SL, Johnson DA, Miltenberger MA, Farzam H. Predicting the service life of concrete marine structures: an environmental methodology. ACI Struct J 1998;95:205–14.
[13] Costa A, Appleton J. Chloride penetration into concrete in marine environment—part II: prediction of long term chloride penetration. Mater Struct 1999;32(5):354–9.
[14] Song HW, Lee CH, Ann KY. Factors influencing chloride transport in concrete structures exposed to marine environments. Cement Concr Compos 2008;30(2):113–21.
[15] Kassir MK, Ghosn M. Chloride-induced corrosion of reinforced concrete bridge decks. Cement Concr Res 2002;32(1):139–43.
[16] Yu H, Sun W, Ma H. Diffusion model of chloride in concrete I—homogeneous and inhomogeneous diffusion in infinite body. J Nanjing Univ Aeronaut Astronaut 2009;41:276–80. Chinese.
[17] Zhang WM, Liu YZ, Xu HZ, Ba HJ. Chloride diffusion coefficient and service life prediction of concrete subjected to repeated loadings. Mag Concr Res 2013;65(3):185–92.
[18] Zhang WM, Ba HJ, Chen SJ. Effect of fly ash and repeated loading on diffusion coefficient in chloride migration test. Constr Build Mater 2011;25(5):2269–74.
[19] Yu H. Study on high performance concrete in salt lake: durability, mechanism and service life prediction [dissertation]. Nanjing: Southeast University; 2004. p. 147–98. Chinese.
[20] Yu H, Sun W, Yan L, Ma H. Study on prediction of concrete service life I—theoretical model. J Chin Ceram Soc 2002;30(6):686–90. Chinese.
[21] Martín-Pérez B, Zibara H, Hooton RD, Thomas M. A study of the effect of chloride binding on service life predictions. Cement Concr Res 2000;30(8):1215–23.
[22] Tuutti K. Corrosion of steel in concrete. Stockholm: Swedish Cement and Concrete Institute; 1982. p. 469–78.
[23] Arya C, Newman JB. An assessment of four methods of determining the free chloride content of concrete. Mater Struct 1990;5(5):319–30.
[24] Mohammed TU, Hamada H. Relationship between free chloride and total chloride contents in concrete. Cement Concr Res 2003;33(9):1487–90.
[25] Thomas M, Bamforth PB. Modelling chloride diffusion in concrete–effect of fly ash and slag. Cement Concr Res 1999;29(4):487–95.
[26] Xu Z, Ma H, Yu H, Xu M, Xu Y, Feng T. Time variation law of free chlorine ion content in the surface of marine concrete structure and its influence on life. Ocean Eng 2017;35:126–34. Chinese.
[27] Yu H. ChaDuraLife V1.0. Nanjing, China: Nanjing University of Aeronautics and Astronautics; 2015.
[28] Jensen MM, De Weerdt K, Johannesson B, Geiker MR. Use of a multi-species reactive transport model to simulate chloride ingress in mortar exposed to NaCl solution or sea-water. Comput Mater Sci 2015;105:75–82.
[29] Liu QF, Iqbal MF, Yang J, Lu X, Zhang P, Rauf M. Prediction of chloride diffusivity in concrete using artificial neural network: modelling and performance evaluation. Constr Build Mater 2021;268:121082.
[30] Liu QF, Easterbrook D, Yang J, Li L. A three-phase, multi-component ionic transport model for simulation of chloride penetration in concrete. Eng Struct 2015;86:122–33.
[31] Ministry of Housing and Urban–Rural Developments of the People's Republic of China, General Administration of Quality Supervision, Inspection and Quarantine of the People's Republic of China. GB/T 50081–2002: Standard for test method of mechanical properties on ordinary concrete. Chinese standard. Beijing: China National Standard; 2003.

[32] Ministry of Transport of the People's Republic of China. JTJ270–98: Testing code of concrete for port and waterwog engineering. Chinese standard. Beijing: China National Standard; 1998.
[33] Yu H, Sun W, Ma H. Diffusion model of chloride in concrete II–homogeneous and inhomogeneous diffusion in finite body. J Nanjing Univ Aeronaut Astronaut 2009;41:408–13. Chinese.
[34] Yu H, Tan Y, Feng T. Study of temporal change in chloride diffusion coefficient of concrete. ACI Mater J 2019;116(1):103–12.
[35] Leng F, Feng N, Lu X. An experimental study on the properties of resistance to diffusion of chloride ions of fly ash and blast furnace slag concrete. Cement Concr Res 2000;30(6):989–92.
[36] Yu B, Ma Q, Huang HC, Chen Z. Probabilistic prediction model for chloride diffusion coefficient of concrete in terms of material parameters. Constr Build Mater 2019;215:941–57.
[37] Sotiriadis K, Rakanta E, Mitzithra ME, Batis G, Tsivilis S. Chloride-related phenomena in limestone cement materials: effect of mineral admixtures and sulfates. ACI Mater J 2019;116(6):19–30.
[38] Angst U, Elsener B, Larsen CK, Vennesland O. Critical chloride content in reinforced concrete—a review. Cement Concr Res 2009;39(12):1122–38.
[39] Jin Z, Zhao T, Hou B, Li Q. Service life prediction of lining concrete for Jiaozhou bay subsea tunnel. J Civil Arch Environ Eng 2009;31:86–91. Chinese.
[40] Wang S, Li K, Fan Z, Su Q, Xiong J. Durability strategy for main concrete structure of Hong Kong–Zhuhai–Macao bridge with designed service life of 120 years. Port Waterway Eng 2015;3:78–84. Chinese.
[41] Raupach M. Investigations on the influence of oxygen on corrosion of steel in concrete—part 1. Mater Struct 1996;29(3):174–84.
[42] Raupach M. Investigations on the influence of oxygen on corrosion of steel in concrete—part 2. Mater Struct 1996;29(4):226–32.
[43] Feng T. Durability assessment and service life design of Dalian Bay immersed tunnel [dissertation]. Nanjing: Nanjing University of Aeronautics and Astronautics; 2017. p. 19–22. Chinese.
[44] Xu M. Study on durability of concrete in Dalian port and time-dependent law of chloride diffusion coefficient [dissertation]. Nanjing: Nanjing University of Aeronautics and Astronautics; 2017. p. 50–71. Chinese.
[45] Keiki M, Shigerou I, Run T, Hiroshi O. Investigation on the durability of concrete structures in Okinawa County. Proc Concrete Eng 2001;23:1177–82. Japanese.
[46] Yi AY, Chuki K, Saka S. The degradation process of RC structure in salt environment. Annu Rep Concrete Eng 1994;16:947–52. Japanese.
[47] Moribe A, Isaka K, Tsutomu F, Takashi B. Durability of reinforced concrete structures subjected to tidal zone and in the sea more than 70 years. Summ Annu Paper Eng Res 1997;19:829–34. Japanese.
[48] Liu W, Zhu C, Han Y. Study on steel bar rust caused by chloride diffusion in concrete. J Waterway Harbor 1992;2:30–8. Chinese.
[49] Lv JF, Tan ZJ, Ba HJ. Micro-structure and performance analysis of marine concrete after extended exposure to marine environment. J China Univ Min Technol 2010;39:528–33. Chinese.
[50] Toru Y, Matsuo N, Hamada H, Yifu Y. Investigation results on the performance of concrete under actual ocean environment exposed for long term. J Acad Year 2008;30:609–39. Japanese.
[51] Park DC, Ahn JC. The property evaluation of the marine concrete structure constructed in the period of Japanese occupancy (YoungDo Bridge). J Korean Navigation Port Res 2013;37(2):165–71. Korean.
[52] Endo H, Taguchi F, Shimada H, Hoshi T, Ota T, Sawa N. Evaluation of port concrete structures in Hokkaido from 10 years to 40 years. J Japan Soc Civ Eng 2008;64:484–99. Japanese.
[53] Kim HS, Kim CG, Na WB, Kim JK. Chemical degradation characteristics of reinforced concrete reefs in South Korea. Ocean Eng 2008;35(8–9):738–48.
[54] Gjørv OE. Durability design of concrete structures in the severe environments. New York: Taylor & Francis Group; 2009.
[55] Ferreira M, Jalali S. Software for probability-based durability analysis of concrete structures. In: Alexander MG, Beushausen HD, Dehn F, Moyo P, editors. Concrete Repair, Rehabilitation and Retrofitting. London: Taylor & Francis Group; 2006.
[56] Ferreira RM. Optimization of RC structure performance in marine environment. Eng Struct 2010;32(5):1489–94.
[57] Ma YL, Zhang AL. Durability life prediction of concrete structure based on the regulated reliability index under chloride environment. Chin Civil Eng J 2006;39:36–41. Chinese.
[58] Trevor JK, Weyers RE, Sprinkel MM, Anderson-Cook CM. Impact of specification changes on chloride induced corrosion service life of Virginia bridge decks. Cem Concr Res 2002;32(8):1189–97.
[59] Kwon SJ, Na UJ, Park SS, Jung SH. Service life prediction of concrete wharves with early-aged crack: probabilistic approach for chloride diffusion. Struct Saf 2009;31(1):75–83.
[60] Li K, Li Q, Wang P, Fan Z. Durability assessment of concrete immersed tube tunnel in Hong Kong–Zhuhai–Macao sea link project. Proceedings of the 27th National Biennial Conference of the Concrete Institute of Australia in conjunction with the 69th RILEM Week; 2015 Aug 30–Sep 2; Melbourne, Australia. Melbourne: Concrete Institute of Australia; 2015.
[61] Ryan PC, O'Connor AJ. Probabilistic analysis of the time to chloride induced corrosion for different self-compacting concretes. Constr Build Mater 2013;47:1106–16.
[62] Lollini F, Carsana M, Gastaldi M, Redaelli E, Bertolini L. The challenge of the performance-based approach for the design of reinforced concrete structures in chloride bearing environment. Constr Build Mater 2015;79:245–54.
[63] Rahimi A, Gehlen C, Reschke T, Westendarp A. Approaches for modelling the residual service life of marine concrete structures. Int J Corros 2014;2014:1–11.
[64] Duprat F. Reliability of RC beams under chloride-ingress. Constr Build Mater 2007;21(8):1605–16.
[65] Jin W, Yuan Y, Wei J, Wang H. Durability theory and design method of concrete structures in chloride environment. Beijing: Science Press; 2011. Chinese.
[66] Gehlen C, Schiessl P. Probability-based durability design for the Western Scheldt Tunnel. Struct Concr 1999;2:1–7.
[67] Zheng SH. Study on service life prediction of Xiang'an tunnel. Proceedings of the first underwater tunnel construction and management technology exchange meeting. Nanjing, China. Beijing: China Highway and Transportation Society; 2013 Nov 28. Chinese.
[68] Breitenbücher R, Gehlen C, Schiessl P, van den Hoonaard J, Siemes T. Service life design for the Western Scheldt Tunnel. In: Lacasse MA, Vanier DJ, editors. Proceedings of the 8th International Conference on Durability of Building Materials and Components, Workshop on Information Technology in Construction; 1999 May 30–Jun 3; Vancouver, Canada. Ottawa: NRC Research Press; 1999. p. 3–15.
[69] Ministry of Transport of the People's Republic of China. JTG/T B07-01–2006: Specifications for deterioration prevention of highway concrete structures. Chinese standard. Beijing: China National Standard; 2006.
[70] Ministry of Transport of the People's Republic of China. JTS151–2011: Design code for concrete structures of port and waterway engineering. Chinese standard. Beijing: China National Standard; 2011.